Creating a SEP Kick Stage Assisted Saturn Trajectory

Josef Biberstein, Andrew DeNucci, Charlie Garcia, Lucy Halperin, Bradley Jomard, David Mueller, Devansh Agrawal*
Massachusetts Institute of Technology, Cambridge, MA, 02139

I. Abstract - Lucy

Missions to outer planets and their moons require complex trajectory planning to arrive at the target object with reasonable mission duration and at reasonable cost. Innovative types of propulsion, as well as techniques which exploit three body dynamics, can be used to enable such missions. This article focuses on the specific trajectory developed for the Enceladus Life Detection, Exploration and Reconnaissance (ELDER) mission lead by the Massachusetts Institute of Technology Department of Aeronautics and Astronautics. A solar electric propulsion kick stage to get the spacecraft from Earth to Venus, a ballistic trajectory to get the spacecraft from Venus to the Saturnian system, and moon tours within the Saturnian system to arrive at Enceladus and to dispose of the spacecraft upon mission completion are described. Use of NASA's General Mission Analysis Tool to simulate the end-to-end mission dynamics is explained. The launch window found for the aforementioned trajectory is given, as are suggestions for how to diversify potential launch windows and use other three body techniques to decrease mission cost.

II. Introduction - Lucy

The department of Aeronautics and Astronautics at the Massachusetts Institute of Technology endeavored to conceive and design an Ocean World Mission to detect life on another body within the Solar System. An Enceladus orbiter (coined ELDER) was selected for the mission due to Enceladus' combined relative ease of accessibility and likelihood of providing evidence for life. ELDER's Launch, Navigation, Entry, Descent, and Landing (LNEDL) team was tasked with planning end-to-end mission dynamics, orbital mechanics, and spacecraft delivery to Enceladus.

Due to the changing nature of the solar system (bodies are constantly varying their relative positions), trajectories from previous missions to the Saturnian system cannot be exactly replicated for new missions. Various interplanetary transfer techniques such as gravity assists and trajectory correction maneuvers must be combined in new ways to ensure a successful operation. Literature detailing theoretical trajectories within the Saturnian system and actual trajectories used in past missions to Saturn were studied to provide ideas for the ELDER mission. The trajectory of NASA's Cassini mission to Titan (a Venus-Venus-Earth-Jupiter gravity assist) became the baseline for ELDER's journey to the Saturnian system. Moon tour concepts detailed in the work of Strange et al. [1] laid the groundwork for ELDER's flight path within the Saturnian system.

Ideas from the aforementioned mission and paper as well as novel uses of solar electric propulsion are joined to develop a viable flight path for the ELDER mission. In this paper, we detail the trajectories required for ELDER's three main mission stages (interplanetary flight from Earth to Enceladus, orbit at Enceladus, and end-of-life spacecraft disposal) and the techniques used to enable the trajectories. Additionally, we cover our utilization of NASA's General Mission Analysis Tool to aid in developing the selected trajectories and suggestions for new strategies to produce end-to-end dynamics for future missions to outer planets.

III. Experimental Design

A. Motivation for Solar Electric Phase - Charlie

The ELDER mission was envisioned as a Discovery Class mission, which constrains the total mass, complexity, and cost of the mission. It also motivates flying on cheaper launch vehicles. Direct-Saturn trajectories are very energy

*Department of Aeronautics and Astronautics

intensive, all missions to Saturn so far have used gravity assists from inner planets and Jupiter to reach Saturn. This trajectory still requires a significant escape velocity from Earth, which means that the payload mass is still constrained, to well below 1000kg, which prevents us from achieving our science objectives. Since previous missions to Saturn, electric propulsion has been developed significantly. Electric propulsion is far more efficient at delivering payload mass to high energy orbits than the upper stage of a launch vehicle, due to it's higher c^* and lower dry mass than an upper stage. If the spacecraft utilizes an inner solar system flyby additional synergies exist, as the spacecraft can use much more mass efficient solar panels to power the electric propulsion system, allowing it to use much more electric thrust than would be enabled by the radioisotope generator units on the spacecraft.

The novel combination of solar propulsion in the inner solar system and chemical propulsion for maneuvering in the Saturnian system enables significantly more payload mass to be delivered, with 3000kg of mass available using the SEP vs 900 kg using the upper stage of a launch vehicle.

This create new challenges for trajectory designs as correctly designed flybys have very narrow gates that are challenging to target with low thrust propulsion. This motivates work into solving for acceptable trajectories while using the low thrust SEP Kick Stage.

B. Electric Propulsion Trajectory Design - Devansh

Traditional trajectory design often assumes a series of short, impulsive burns are performed. This is not acceptable for a continuous low thrust maneuvers as in the electric descent to Venus. To determine the ΔV needed for this maneuver, the problem is set up as an optimization problem.

$$\max_{T(t)} m(t_f) \tag{1}$$

subject to the dynamics,start and end conditions, and maximum thrust constraints $||T(t)|| < T_max$, where $m(t)$ is the spacecraft mass as a function of time, and t_f is the final time for this simulation, the arrival time at Venus.

The problem is simplified by assuming all orbits are planar, reducing the problem to finding the 2D path about the Sun. It is also assumed that only gravitational force is due to the Sun, and the gravitational effects close to the Earth and Venus were ignored. The state is described using 5 elements,

$$x = [r, v_r, v_\theta, m, \theta] \tag{2}$$

where r is the radial distance from the sun, v_r, v_θ describe the radial and tangential velocity vectors in heliocentric coordinates, m is the mass and θ is the angular position of the spacecraft in heliocentric coordinates. The dynamics are described by

$$\dot{r} = v_r \tag{3}$$

$$\dot{v_r} = \frac{v_\theta^2}{r} - \frac{\mu}{r} + \frac{T_r}{m} \tag{4}$$

$$\dot{v_\theta} = -\frac{v_\theta v_r}{r} + \frac{T_\theta}{m} \tag{5}$$

$$\dot{m} = -\frac{\sqrt{T_r^2 + T_\theta^2}}{c} \tag{6}$$

$$\dot{\theta} = \frac{v_\theta}{r} \tag{7}$$

where the control input is a 2 element vector $u = [T_r T_\theta]$ describing the radial and tangential components of thrust.

To solve the optimal control problem, a Pseudo-spectral method is used, where the problem is discretized using Legendre–Gauss–Radau points, and then the a non-linear optimizer is used to find the optimal control inputs. The problem was solved using the open source package openGoddard [2].

C. Designing the Interplanetary Flyby Sequence - David

Initially, determining the timeline for the entire sequence of interplanetary transfer orbits is accomplished by constraining a target arrival epoch at Saturn, then determining potential transfer orbits to that point and epoch from

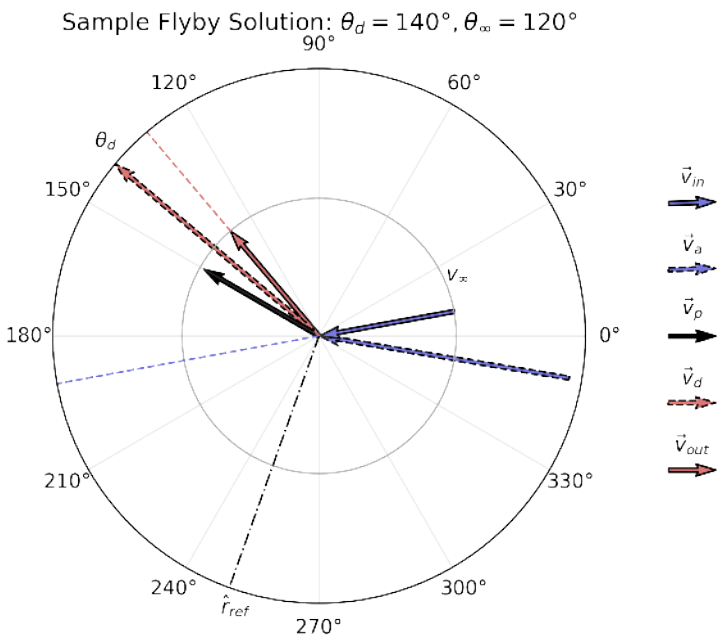

Fig. 1 Example flyby solution plot, showing approach and departure sun-relative velocities $\vec{v}_a$ and $\vec{v}_d$, to and from the flyby target planet, respectively. These velocities are also shown relative to the moving planet-centered frame, $\vec{v}_p$, as $\vec{v}_{\text{in}}$ and $\vec{v}_{\text{out}}$. The free parameter θ_∞ defines the angle between $\vec{v}_{\text{out}}$ and $\hat{r}_{\text{ref}}$.

Jupiter by solving Lambert's problem. Lambert's problem deals with finding an orbit such that a body in that orbit will pass through 2 specified points, with a specified elapsed time to move between them. However, this approach has a major drawback: since Lambert's problem places no constraints on the velocities of the resulting orbit, simply guessing start and end epochs typically results in unobtainable velocities. Because of this limitation, better techniques are needed to converge on a family of solutions.

The new technique used for this project uses the known flyby departure vector $\vec{v}_d$ and its motion relative to the moving planet $\vec{v}_p$ to define the planet-relative outbound velocity vector:

$$\text{outbound velocity} \coloneqq \vec{v}_{\text{out}} = \vec{v}_d - \vec{v}_p \tag{8}$$

where $\vec{v}_{\text{out}}$ is aligned with the outbound asymptote of a hyperbolic flyby trajectory.

The angle between $\vec{v}_{\text{out}}$ and the hyperbola's major axis, $\hat{r}_{\text{ref}}$, is defined as θ_∞ and is a free parameter. $\vec{v}_{\text{out}}$ and θ_∞ constrain the inbound velocity vector $\vec{v}_{\text{in}}$ to a single value, thus making $\vec{v}_{\text{in}}$ a function of θ_∞ when $\vec{v}_{\text{out}}$ is held constant. The geometric arrangement of these elements is visualized in Figure 1. $\vec{v}_{\text{in}} + \vec{v}_p$ then uniquely defines an orbit which can be back-propagated to determine if it encounters the previous planet.

Thus, for each flyby, θ_∞ can be varied to find transfer orbits from the previous planet, as can be seen by comparing Figures 1 and 2. The advantage this provides over solving Lambert's problem is that every resulting trajectory is *also* guaranteed to result in the desired flyby. More information about this technique is provided in VI.CAppendix A.

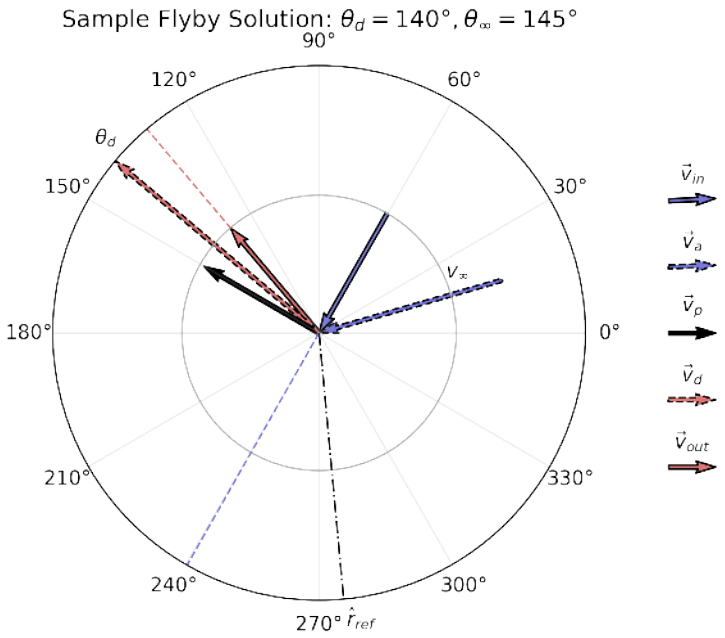

Fig. 2 Another solution for the same departure trajectory as Figure 1, plotted at the same scale. Note the reduced $\|\vec{v}_a\|$ and larger turning angle, ψ, from $\vec{v}_{\text{in}}$ to $\vec{v}_{\text{out}}$. $\|\vec{v}_a\|$ and ψ are both functions of θ_∞.

D. GMAT Simulation - Josef

The NASA General Mission Analysis Tool (GMAT) is a high fidelity tool for space mission design and physical propagation of spacecraft under gravitational and aerodynamic forces. Developed by NASA, this tool is an open source alternative to more expensive closed source software such as the Systems Tool Kit (STK). GMAT has been used as the primary mission planning tool for a number of flown missions, including TESS. GMAT provides the ability to propagate spacecraft subject to gravitational forces in the solar system. The default version simulates all eight major planets plus Pluto, Luna and Sol with capability to create arbitrary other bodies and automatically add realistic orbital parameters using JPL SPICE toolkit files. GMAT provides the capability to target sets of orbital conditions by allowing the mission planner to vary parameters such as initial orbital elements, duration and magnitude of finite or impulsive burns, and propagation times in order to achieve a desired end state after a series of propagations.

For the simulation of the ELDER mission's trajectory, we began by defining orbital parameters and masses for Titan and Enceladus using GMATs SPICE toolkit integration. This allowed us to take the gravity and motion of these bodies into account in the simulation. We also defined a the ELDER spacecraft in the GMAT simulation, entering accurate esitmates of the spacecraft mass provided by the bus design team. We then developed the following simulation plan.

1) Beginning at Earth, we position ELDER in an exit orbit with a C3 of $12 m^2/s^2$.
2) Using a targeter, we vary the starting inclination of the exit orbit from Earth to allow us to obtain the correct inclination to intersect with Venus orbit.
3) We allow the simulation to propagate until Jan. 8 2041, the required date to be at venus in order to execute the Venus-Earth-Jupiter-Saturn gravity assist (VEJSGA). As we propegate to this date, we make four solar orbits. At the apoapsis of these orbits, we burn retrograde with electric thrusters for a variable amount of time chosen by the targeter but informed by the optimal control solutions for minimizing ΔV required to bring our orbital periapsis to the radius of the Venus orbit.
4) Running the described targeter, we achieve a set of b-plane parameters at Venus which put us in the correct orbit to take advantage of the VEJSGA.
5) After arriving at Venus and achieveing the correct orbit, we decrease the mass of the spacecraft to reflect jetisoning the electric kick stage.
6) We begin a new targeter that varys the magnitude of a small impulsive burn at Venus to allow small trajectory adjustments for the VEJSGA.

7) We then propegate to Earth, Jupiter, and Saturn periapsis in turn. As we near each planet, we change the propagator to one specialized for the sphere of influence of each body to increase accuracy.
8) Finally, we achieve orbital insertion radius at Saturn. A small breaking burn is performed to capture into Saturn orbit.

In summary, the trajectory is divided into two sections - the journey to Venus via the electric kick stage and the VEJSGA trajectory. Thus we can simulate each part of the trajectory separately and then match the end conditions of the first part with the desired start conditions of the second part. Once the full trajectory is simulated, we can obtain the ΔV required to make the journey from GMAT. GMAT provides detailed reports of the spacecraft state at each simulation event in any given coordinate frame. This state includes ΔV information.

E. Moon Tour-Andrew, Bradley

Upon arrival at Saturn, the first step will be to capture into Saturnian orbit. With the small amount of ΔV available, a direct capture to Enceladus is untenable (ΔV = 6.30 km/s), and even leveraging a gravity assist from Titan alone, Saturn's largest moon, is prohibitively expensive (ΔV = 3.57 km/s). Therefore the spacecraft will enter the Saturnian system between the F and G rings, and capture into a highly elliptical orbit with apoapsis of 200 Saturn radii and periapsis of 1.2 Saturn radii.

Once the initial orbit is achieved, the spacecraft will need to shed velocity in order to perform Enceladus orbit insertion (EOI). Because every kg of fuel used for this final series of burns will increase the cost of all the previous burns, we are to 1500 m/s propulsive ΔV for Saturn orbit insertion (SOI), transit to Enceladus, EOI, and spacecraft disposal. Consequently, this phase of the mission relies heavily on gravity assists. Starting at Titan, Saturn's most massive moon, the spacecraft will perform flybys of four moons, moving progressively inwards in the Saturnian system until it encounters Enceladus. To begin the moon tour, we will need to raise the periapsis of the initial capture orbit to be able to intersect with Titan's orbit. This will be done with a burn at the orbits apoapsis.

The Lambert's solver method described must be adapted for this endgame problem, as the moons of Saturn are not massive enough for a single flyby to apply sufficient ΔV to lead to a rendezvous with the next moon inwards. Literature review suggested that aside from Titan, each moon would require between 10 to 15 flybys [3]. With such a large solution space, we turn to a graphical method to increase the tractability of the problem. This approach, introduced by Strange and Longuski [4], utilizes Tisserand's parameter, a quantity that is conserved in the restricted three-body problem, to plot sets of orbits. Presented on T-r_p axes, orbits are organized into contours of constant v-infinity relative to a moon. A single orbit is thus a single point on a contour, defined by its interacting body, v_{infty}, period, periapsis distance, and a final parameter called the pump angle, α. As depicted in 3, this is the angle between exit velocity and the moon's velocity. Transfer opportunities are represented by overlaps in the contours, as the orbit in question interacts crosses the path of multiple moons. The objective with these plots is thus to trace a continuous path along contours until a low v-infinity contour associated with the destination is reached and an insertion maneuver can be executed. Once a viable

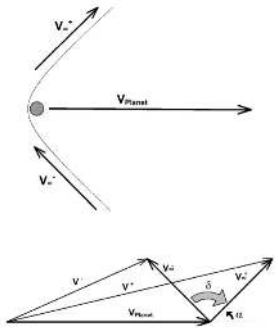

Fig. 3 In a flyby, the spacecraft's velocity to the body, v_∞, is constant

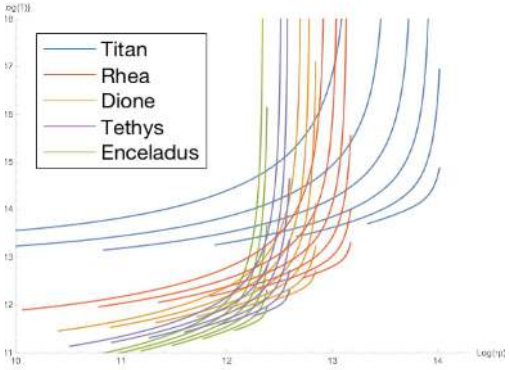

Fig. 4 The Saturn system presents abundant flyby opportunities.

tour is identified, each flyby is calculated. On each contour, the spacecraft must change its orbit by some $\Delta\alpha_{total}$ in

order to rendezvous with the next body. Flybys have a maximum $\Delta\alpha_{max}$

$$\Delta\alpha_{max} = 2\arcsin\left(\frac{1}{1 + (r_p + l_{min})(\frac{v_\infty^2}{\mu})}\right)$$

where l_{min} is the minimum flyby altitude. An optimization problem is thus introduced, where we seek to minimize the spacecraft time of flight, subject to the constraint that the sum of all the flybys' $\Delta\alpha$ is equal to $\Delta\alpha_{total}$. A useful heuristic is to only consider $\Delta\alpha$ values that result in orbits with a resonance with the moon, to ensure a future gravity assist and simplify computation.

To further decrease the duration of the trip, Strange, Campagnola, and Russell introduce the method of V-Infinity Leveraging Transfers (VILT) to the analysis[1]. With a small impulsive maneuver, VILT's can achieve large changes in v-infinity, as well as improve the orbital resonance (eg. from 19:18 to 1:1), leading to a shorter overall time of flight. In analysis, it is assumed that VIL maneuvers will be applied at either periapsis (interior leveraging) or at apoapsis (exterior leveraging). Using nondimensionalized quantities, the group derives a method that allows for the computation of a VILT, as well as a computation to satisfy the phasing requirement that constrains the free parameter. This computation requires the iterative guessing of phase-free VILTs until the constraint, so the process can be slow and non-optimal.

The same group introduces a faster method that utilizes a linear approximation of the problem, which allows for a broader search. The optimal linear trajectory is then recomputed with the nonlinear model, with a small difference in total ΔV [5]. It is an approach similar to using a branch and bound approach with linear programming to solve an integer programming problem. It makes a complicated problem more tractable by solving many simpler sub-problems, then checking against the real model.

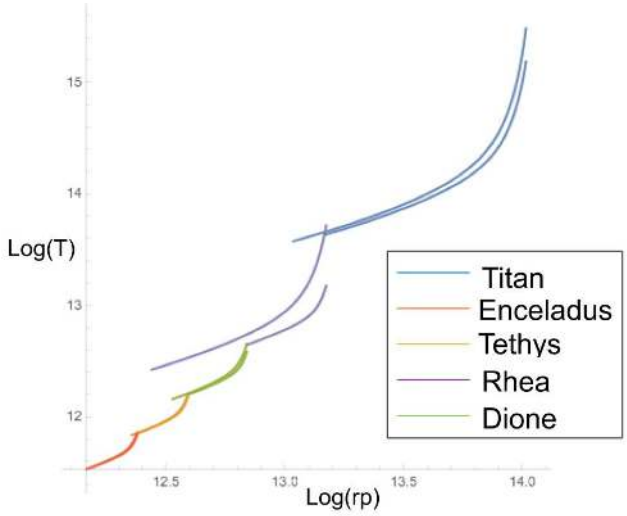

Fig. 5 By changing v_∞ contours between flybys of the same body, the tour can arrive at Enceladus with a lower velocity. Depicted are the initial and final contours of each tour segment.

Once we completed the full moon tour, putting us at Enceladus, we will need to capture into the proper orbit to allow the spacecraft to perform the measurements needed for mission success. To do this we will be targeting a capture at the poles, and perform a retrograde burn to slow down and capture into a polar orbit that is initially 100km off the surface of Enceladus. From there, we will be progressively lowering the orbit from 100km to 20km with small burns to be able to take measurements closer into the plumes, based on requests from the science team.

Similar analysis was performed for spacecraft disposal. Multiple flybys of Enceladus and Saturn's moon Mimas will allow the spacecraft to move progressively inwards towards Saturn. Ultimately, the spacecraft will crash into Saturn and thus comply with NASA planetary protection rules. Impacting Enceladus is also supported in the literature, if the impact occurs outside of 55-90 degrees latitude in the south polar region [3].

IV. Results

A. Overview - Charlie

The trajectory occurs in three phases. An initial orbit lower occurs using solar electric propulsion to obtain an initial Venus fly-by. After the first Venus fly-by the SEP stage is jettisoned and the spacecraft follows a ballistic outbound trajectory utilizing a second Venus fly-by, an Earth fly-by, a Jupiter fly-by, before finally arriving at Saturn. After arriving at Saturn a series of moon fly-bys will lower the orbit to Enceladus where a final propulsive maneuver will capture ELDER in a polar Enceladus orbit.

B. Results of SEP trajectory optimization - Devansh

Figure 6 shows two electric propulsion trajectories that will launch from Earth and arrive at Venus with the correct phasing. The arrows indicate the thrust direction and relative magnitude. The left trajectory requires a higher C3 and less xenon than the right trajectory. The transfer duration can be controlled to some degree, but will cost fuel. The spacecraft was designed for a $\Delta V = 7$ km/s to allow for some margin. Both trajectories end with the relative to Venus that is required to set up the flyby tour.

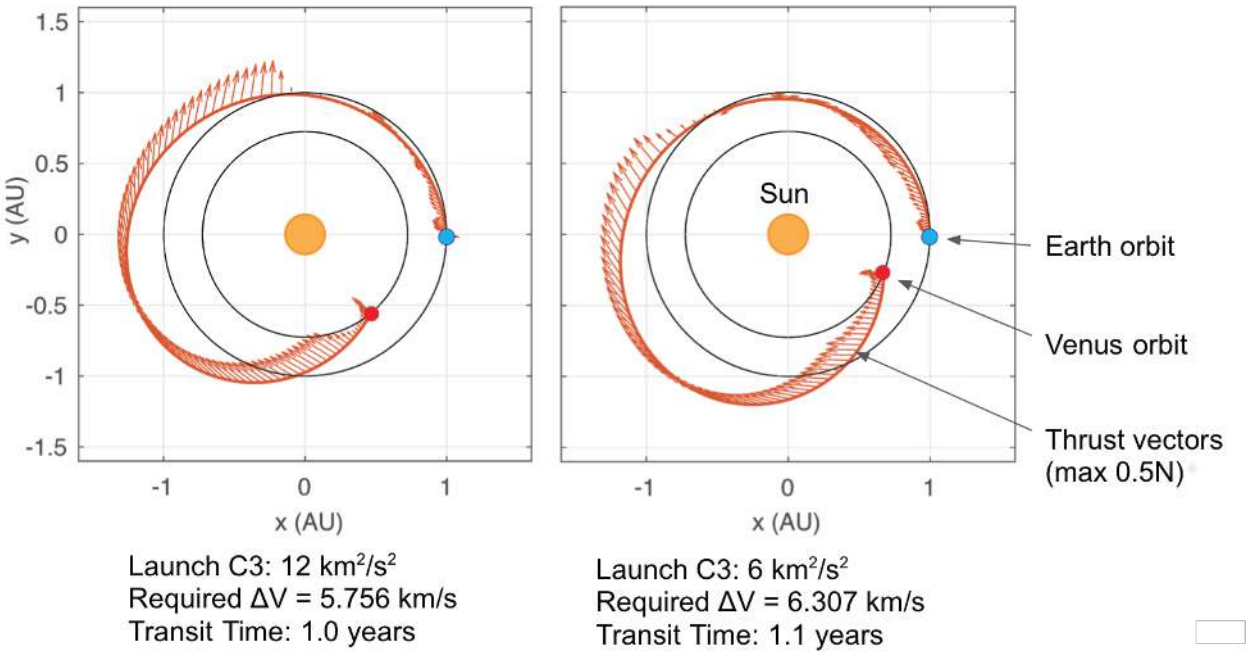

Fig. 6 Two possible trajectories for Earth-Venus transfer. Arrows indicate thrust force.

C. Results of VEJS Gravity Assist Windows - David

Even with the desirable constraints gained though use of the techniques discussed in section III.C, the flyby trajectory is still a chaotic system problem with 6 degrees of freedom. To address the difficulties in fining optimal solutions for this dynamical system, two numerical optimization methods were considered due to their availability in the SciPi Python package [6], and for their suitability for use with boundary constraints and other general constraints: the Constrained Optimization BY Linear Approximation (COBYLA) method [7], and Sequential Least Squares Programming [8].

After attempting use of both methods, Sequential Least Squares was found to be far more suitable for this particular problem. This is because, although COBYLA consistently ran its optimization routines much faster – roughly an order of magnitude faster – the algorithm itself does not strictly adhere to the boundary conditions specified by the programmer, by design. This proved to be problematic, due to heavy reliance on a physics propagator, which requires strict adherence to causality. The optimization routine minimizes the required energy on arrival at Venus, which in turn, minimizes the propellant required from the SEP kick stage. The results of this optimization are shown in 1.

D. Results of Saturn Orbit Insertion and Moon Tour-Andrew

Two moon tour possibilities were identified by Campagnola, Strange, and Russell [1],[5]. One design requires $316m/s$ ΔV and 2.7 years, while the other requires $492m/s$ and 2.0 years. See Table 1 for a full comparison. Ultimately, the longer tour was selected for the mission, as the extra propellant outweighed the longer trip duration, as there was still enough time to complete the baseline mission, and even accommodate a possible mission extension. There are 52 flybys in total. Table 2 gives an entire breakdown of the tour including 3 at Titan, 15 at Rhea, 10 at Dione, 12 at Tethys, and 12 at Enceladus.

In order to utilize the chosen moon tour, the spacecraft needs to be captured into an orbit with a v_∞ at Titan of $1.46km/s$. To do so, we enter the system between the F and G rings as the Cassini mission did, then enter into an initial orbit recommended by the Titan Saturn System Mission [4], which has periapsis at 1.2 Saturn radii and a $772m/s$ burn to close the orbit with a apoapsis at 200 Saturn radii. In order to compute the correct periapsis raise maneuver (PRM) to match the desired v_∞, we use a variation of the VILT method presented in [1]. The PRM comes out to an additional $192m/s$ to raise the periapsis to 4.76 Saturn radii. After expending 316 m/s during the tour, along with the recommended 5m/s ΔV margin per flyby, the spacecraft executes a $128m/s$ burn, leaving $432m/s$ worth of propellant for the end of the mission. $128m/s$ of that propellant will be used to capture at Enceladus. Ultimately, the spacecraft will $436m/s$ ΔV remaining for science operations and disposal.

E. Mission ΔV - Charlie

The mission expends approximately $5.5km/s$ over the duration of the mission. Orbit lowering using solar electric propulsion will expend $4.1km/s$. The spacecraft will then expend $722m/s$ to capture at Saturn. The remainder of the ΔV will be expended doing maneuvers to fly the moon intercept trajectories and conducting science maneuvers.

There is a period of time around the nominal launch date which offers similar transit times for similar ΔV. Figure 7 shows the opportunities to mitigate launch date slip. The ΔV varies minimally, as does the first Venus flyby date. Launch slips greater than 30 days can be accommodated by sacrificing some missed-thrust opportunities.

ΔV expenditures in the Saturnian system consist of propusively assisted flybys of 5 moons a total of 15 times. The ΔV expenditure at each moon is listed in Table **??**.

The final capture burn at Encleadus is a further 128 m/s. Stochastic pertubations by other moons in the Saturnian system preclude any orbit around Enceladus with an inclination of greater than 66° degrees from being stable [9]. This requires between 42 m/s and 65 m/s per year to perform orbital maintenance.

F. Mission Duration - Charlie

The SEP phase will less than two solar orbits if two Hall Effect thrusters remain operational with less than 30% missed thrust, with contingency orbit lowering in the event of a thruster failure requiring either less missed thrust, or additional thrusting. The launch will occur between December 3, 2039 and January 28, 2040. ELDER will begin it's outbound tour on January 8, 2041 with it's first Venus flyby. In March of 2048 Elder will arrive at Saturn and capture into a highly eccentric orbit. In January of 2051 the ELDER spacecraft will perform a breaking burn to capture into a polar orbit above Enceladus and begin its science mission.

G. GMAT Results - Josef

Both the first and second parts of the desired trajectory were independently simulated and achieved the desired orbital parameter end states. However, due to an oversight in our Lambert's problem solutions for the roughing pass at the VEJSGA, the January 8th, 2041 trajectory we picked required a C3 at Venus that was unobtainable (around $200m^2/s^2$ to complete the VEJSGA). Therefore we were not able to achieve an orbital state that would effectively link the two parts of the trajectory for a gravity assist on this date. However, the success of the mission parts individually shows that this simulation plan is sound.

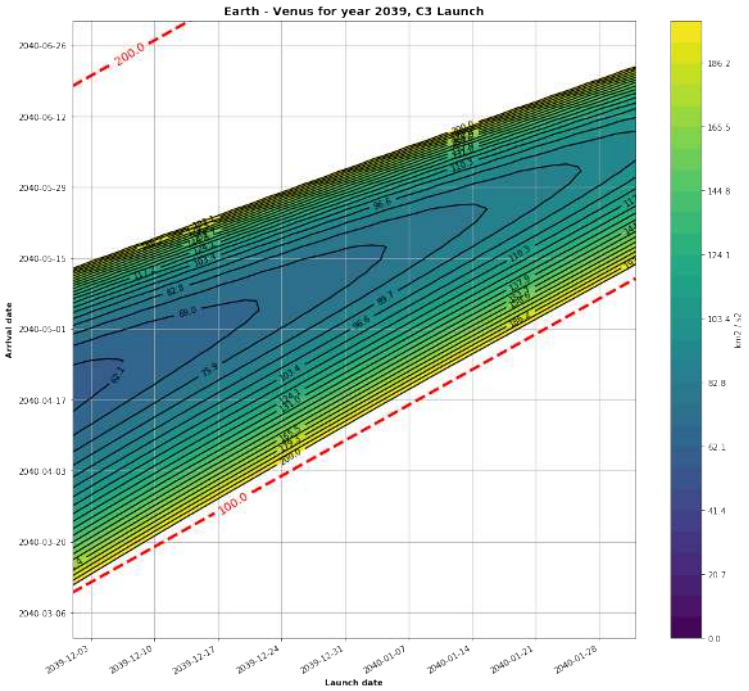

Fig. 7 Departure Date, Venus 1 Arrival Date, and Impulsive ΔV

Body	TCM ΔV
Titan	29 m/s
Rhea	146 m/s
Dione	26 m/s
Tethys	12 m/s
Enceladus	102 m/s

V. Discussion

VI. Conclusions and Future Work

A. Summary- Josef

The trajectory architecture proposed in this article - solar electric propulsion (SEP) kick stage followed by ballistic gravity assist trajectory - has been shown here to be a promising strategy for low cost missions to the outer planets. While we were not able to close a specific trajectory, we were able to promisingly demonstrate that trajectories consummate with this architecture do exist for a spacecraft with ELDER's capabilities. Furthermore, the SEP kick stage offers the possibility of interesting extended missions or even permanent infrastructure - for instance, the kick stage could be designed to remain in solar orbit after being jettisoned and be used repeatedly by other low cost spacecraft to achieve similar trajectories to that described in this article. However, to close the trajectory for the ELDER spacecraft, additional investigation into alternate gravity assist launch windows must be completed. In addition, invariant manifold trajectory design methods may be used to decrease the ΔV required to complete the trajectory.

B. Launch Window Density - Charlie, David

While the trajectory presented in this paper is a valid trajectory, it is only valuable to a mission ready to be launched at the end of the 2030's. Other trajectory opportunities were identified in the process of developing this mission, which were unsuitable for ELDER for a variety of reasons, but they may be useful to future missions. As previously mentioned, a strong emphasis was put on finding a wider variety of flyby trajectories, both for the sake of earlier launch opportunities and greater robustness to launch delays. Preliminary results from these efforts reveal that a wider variety of launch windows may exist, and the same techniques may reveal much sooner launch dates that can take advantage of the SEP architecture. An early result of these findings is shown in Table 1, and further work will likely unveil additional launch opportunities.

Trajectories with perfect alignment opportunities are highlighted in Fig 8. Trajectories are available in families separated by 7 decades. The separation is due to Jupiter-Saturn phasing, which is not necessarily a strong constraint.

C. Non-Keplarian Orbits

This trajectory design end-to-end uses only keplerian orbits, meaning the orbits are concerned with the gravity from a single body and thus follow Kepler's laws. When the gravity of additional bodies is introduced into the analysis, the systems behavior changes dramatically. The computation of such trajectories is intensive, as no analytical solution exists for the n-body problem when $n > 2$. There are ways in which these complex orbits could further enable the ELDER mission. The spacecraft could capture into a halo orbit, for example, that has polar access with greater stability than an polar Enceladus Orbit, or perhaps a ballistic capture trajectory could be designed to mitigate the ΔV required for SOI while also relaxing the tight launch window constraints the mission currently faces[10], [11]. The development of a moon tour employing non-keplerian orbits is an active area of research[12].

Appendix

Appendix A

This attachment describes, with further explanation and justification, the experimental technique mentioned in this memo.

The technique assumes nearly all motion occurs in the invariant plane of the Solar System, and all vectors and orbits are projected onto this plane for these calculations. Derivations are based on first principles and concepts from orbital mechanics as covered in 16.07-Dynamics [13].

The relation between the approach and departure vectors of a flyby stems from the trajectory's hyperbolic shape. As a spacecraft flies into the gravity well of a given planet, it travels on one asymptotic half of a hyperbola at velocity $\vec{v}_{\text{in}}$ with respect to the planet at the focus. Because the departing asymptote must be parallel to the velocity vector needed for the next transfer orbit, $\vec{v}_{\text{out}}$, and the hyperbola's focus is fixed at the planet's barycenter, the hyperbola has a single degree of freedom.

Thus, the shape and orientation of the hyperbola is characterized by the asymptote angle, $\theta_\infty \in (90°, 180°)$. Changing

Venus Epoch	Earth Epoch	Jupiter Epoch	Saturn Epoch	Mean Squared Error (non-dimensional)	Δt_{VE} (days)	Δt_{EJ} (days)	Δt_{JS} (days)
2041-06-09	2041-07-05	2043-02-11	2048-03-10	23877267	25	586	1854
2039-12-03	2040-03-13	2041-11-03	2046-12-03	65236383	101	600	1856
2041-04-29	2041-05-15	2042-11-13	2047-12-18	174875418	16	547	1862
2041-05-23	2041-06-06	2042-12-28	2048-01-19	185005149	14	569	1849
2041-06-27	2041-07-11	2042-12-13	2048-09-07	224834995	14	520	2095
2039-08-17	2039-10-23	2041-06-06	2046-06-28	260287585	67	592	1849
2039-08-31	2040-02-12	2041-10-04	2047-03-26	386054925	165	600	2000
2039-12-04	2040-02-28	2041-10-19	2046-12-07	472252904	86	599	1876
2041-01-18	2041-06-23	2042-10-14	2047-11-27	478803895	156	478	1870
2041-06-11	2041-06-25	2043-01-12	2048-02-02	486534044	14	565	1848
2040-05-27	2040-10-10	2042-05-02	2047-07-04	498709234	137	568	1889
2042-08-03	2042-09-02	2044-03-22	2049-03-29	653878808	30	567	1834
2040-04-22	2040-05-20	2042-01-02	2047-01-14	722364089	28	591	1839

Table 1 A small subset of the optimization algorithm output previously discussed in Section IV.C. This table summarizes the epoch for each encounter at the four target planets, as well as each transfer duration. Note that, at the currently level of fidelity, the mean squared error is still too high, and these trajectories are candidates for further refinement.

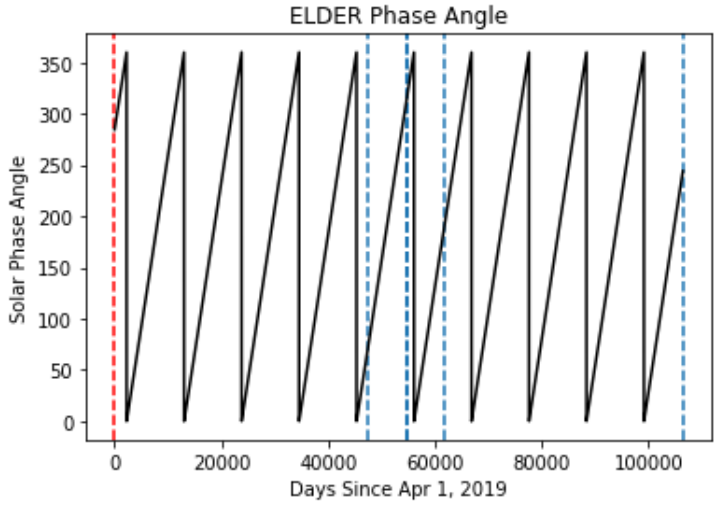

Fig. 8 The phase of Saturn and potential Venus departure dates

this angle dictates the direction of the approach vector, $\vec{v}_a$. Furthermore, because $\vec{v}_{\text{out}}$ also has a fixed magnitude, the magnitude of the approach vector is also fixed. These relations are visualized in Figures 1 and 2.

For any given θ_∞, determining whether the resulting approach transfer trajectory intersects the previous flyby body is relatively simple.

An important limitation not portrayed here the minimum possible θ_∞ for a flyby at a given planet. Since decreasing values of θ_∞ result in closer approaches to the flyby planet, θ_∞ is limited by the radius of the planet and how close of a flyby is deemed acceptable. Equations to derive these limits can be found in Space Mission Analysis and Design[14].

Appendix B

Below is an overview of the entire moon tour.

Titan	TOF [days]	Altitude [km]	vinf [km/s]	vinf' [km/s]	DV [m/s]
1	31.4	2800	1.46	1.26	28.8
2	21.3	3000	1.26	1.26	0
3	--	15090		Transfer	

Rhea	TOF [days]	Altitude [km]	vinf [km/s]	vinf' [km/s]	DV [m/s]
1	9.5	100	1.66	1.68	1.9
2	17.5	2510	1.68	1.67	1.4
3	59.2	60	1.67	1.5	21.5
4	39.1	70	1.5	1.3	25.1
5	22.7	70	1.3	1.2	12.7
6	36.1	270	1.2	1.2	0
7	13.6	150	1.2	1.09	14.6
8	31.7	150	1.09	0.99	15.2
9	40.7	120	0.99	0.9	16.9
10	31.6	230	0.9	0.9	0
11	6.5	220	0.9	0.9	0
12	6.2	310	0.9	0.9	0
13	30.2	60	0.9	0.74	37.2
14	18.1	50	0.74	0.74	0
15	--	3660		Transfer	

Acknowledgments

References

[1] Strange, N., Campagnola, S., and Russell, R., "Leveraging Flybys of Low Mass Moons to Enable An Enceladus Orbiter," , 2009. URL http://citeseerx.ist.psu.edu/viewdoc/download?doi=10.1.1.720.4743&rep=rep1&type=pdf.

[2] Interstellar Technologies Inc., "OpenGoddard," , 2017. URL https://istellartech.github.io/OpenGoddard/.

Dione	TOF [days]	Altitude [km]	vinf [km/s]	vinf' [km/s]	DV [m/s]
1	28	350	0.82	0.78	4.7
2	13.6	270	0.78	0.71	10.3
3	16.5	100	0.71	0.65	9.3
4	24.6	60	0.65	0.64	1.9
5	35.6	960	0.64	0.64	0
6	2.7	120	0.64	0.64	0
7	32.8	60	0.64	0.64	0
8	19.2	190	0.64	0.64	0
9	16.4	970	0.64	0.64	0
10	--	620		Transfer	

Tethys	TOF [days]	Altitude [km]	vinf [km/s]	vinf' [km/s]	DV [m/s]
1	13.4	250	0.7	0.7	0
2	13.2	60	0.7	0.66	6
3	17	60	0.66	0.66	0
4	26.4	70	0.66	0.66	0
5	2.7	60	0.66	0.66	0
6	1.9	640	0.66	0.66	0
7	2.6	610	0.66	0.66	0
8	26.4	80	0.66	0.66	0
9	17	90	0.66	0.66	0
10	13.2	100	0.66	0.66	0
11	24.5	1020	0.66	0.63	6.2
12	--	860		Transfer	

Enceladus	TOF [days]	Altitude [km]	vinf [km/s]	vinf' [km/s]	DV [m/s]
1	27.4	240	0.7	0.7	0
2	9.6	50	0.7	0.7	0
3	20.7	50	0.7	0.74	6.1
4	12.3	50	0.74	0.7	6.5
5	23.3	50	0.7	0.59	19.3
6	12.3	190	0.59	0.59	0
7	13.9	50	0.59	0.56	5.8
8	16.4	50	0.56	0.47	15.1
9	18	50	0.47	0.4	12.5
10	20.5	50	0.4	0.3	16.8
11	25.9	50	0.3	0.22	3.6
12	32.8	50	0.22	0.18	6.4

[3] Spencer, J., and Neiber, C., "Planetary Science Decadal Survey Enceladus Orbiter," , 2010. URL https://ia800308.us.archive.org/9/items/EnceladusOrbiterConceptStudy/22_Enceladus-Orbiter-Final.pdf.

[4] Strange, N., and Longuski, J., "Graphical Method for Gravity-Assist Tour Design," *Journal of Spacecraft and Rockets*, Vol. 39, No. 1, 2002, pp. 9–16. doi:https://doi.org/10.2514/2.3800.

[5] Campagnola, S., Strange, N., and Russel, R., "A Fast Tour Design Method Using Non-Tangent V-Infinity Leveraging Transfers," *Celestial Mechanics and Dynamical Astronomy*, Vol. 108, No. 2, 2010, pp. 165–186.

[6] Jones, E., Oliphant, T., Peterson, P., et al., "SciPy: Open source scientific tools for Python," , 2001–. URL http://www.scipy.org/.

[7] Powell, M., "Direct search algorithms for optimization calculations," *Acta numerica*, Vol. 7, 1998, pp. 287–336.

[8] Powell, M. J., "A view of algorithms for optimization without derivatives," *Mathematics Today-Bulletin of the Institute of Mathematics and its Applications*, Vol. 43, No. 5, 2007, pp. 170–174.

[9] Spencer, J., "Planetary Science Decadal Survey Enceladus Orbiter, Mission Concept Study," , ????

[10] Topputo, F., and Belbruno, E., "Earth–Mars transfers with ballistic capture," *Celestial Mechanics and Dynamical Astronomy*, Vol. 121, No. 4, 2015, pp. 319–346. doi:https://doi.org/10.1007/s10569-015-9605-8.

[11] Russell, R., and Lara, M., "On the design of an Enceladus science orbit," *Acta Astronautica*, Vol. 65, 2009, pp. 27–39. doi:https://doi.org/10.1016/j.actaastro.2009.01.021.

[12] Davis, D. C., Phillips, S., and McCarthy, B., "Trajectory design for Saturnian Ocean Worlds orbiters using multidimensional Poincare maps," *Acta Astronautica*, Vol. 143, 2018, pp. 16–28. doi:https://doi.org/10.1016/j.actaastro.2017.11.004.

[13] Widnall, S., and Peraire, J., "MIT AeroAstro 16.07, Lecture Notes: Orbit Transfers and Interplanetary Trajectories," , 2008. URL https://ocw.mit.edu/courses/aeronautics-and-astronautics/16-07-dynamics-fall-2009/lecture-notes/MIT16_07F09_Lec17.pdf.

[14] "Orbits and Astrodynamics," *Space Mission Analysis and Design*, edited by J. R. Wertz, Microcosm Press, El Segundo, CA, 2009, Chap. 9.6, pp. 231–232.